PERGAMON

International Journal of Heat and Mass Transfer 43 (2000) 577–587

International Journal of HEAT and MASS TRANSFER

www.elsevier.com/locate/ijhmt

Lattice Boltzmann scheme for cooling of packed cut flowers

R.G.M. van der Sman[a,*], M.H. Ernst[b], A.C. Berkenbosch[a]

[a] *Agrotechnological Research Institute, Wageningen, The Netherlands*
[b] *Institute for Theoretical Physics, University of Utrecht, The Netherlands*

Received 6 November 1997; received in revised form 1 April 1999

Abstract

A Lattice Boltzmann scheme is developed for the simulation of the heat and mass transfer during cooling of packed cut flowers. Using this problem as a case study, we investigate whether the Lattice Boltzmann scheme can be used as a generic tool in the design process of packages with agricultural products.

The Lattice Boltzmann method has been chosen for its attractive simplicity and its appeal to physical intuition. The method maps the problem on a regular lattice, populated with lattice gas particles, which move across the lattice and collide with one another.

Mathematical and numerical analysis have shown that our Lattice Boltzmann scheme is consistent with a convection–diffusion equation with heat and mass transfer, even up to high grid Peclet and Courant numbers. Comparison of the simulation results of the LB scheme with experimental data shows that the model applies quite well to cooling of packed cut flowers.

Given the results of this study we conclude that the Lattice Boltzmann scheme is indeed suitable as a generic framework for the modelling of heat and mass transfer processes in packages of agricultural products.

1. Introduction

Many interrelated physical processes play an important role in the heat and mass transfer from packages with agricultural products to the environment, such as conduction, convection, diffusion, respiration, evaporation, condensation, and convective transfer [1,2]. Controlling the heat and mass transfer is crucial for maintaining the keeping quality of the packed products [3]. The barrier properties of packages make them important instruments for controlling the heat and mass transfer. Given the complexity of these processes, a model-based approach of the evaluation of the packaging would greatly enhance the design process.

In large packaging systems, used for road transport and air freight, the spatial variation in physical quantities, such as temperature and density of various gasses (water vapour, O_2, CO_2), can manifest itself in the quality of the packed product. Consequently, the model should describe the spatial distribution of the relevant physical quantities. The mathematical description of these distributions is done with partial differential equations.

Various models have been developed for the description of the heat and mass transfer in packed or stored agricultural products [2–7]. To our knowledge all these models are solved numerically by either a Finite Difference method or a Finite Element method.

* Corresponding author.

0017-9310/00/$ - see front matter
PII: S0017-9310(99)00156-8

Nomenclature

Symbols of PDE model

a	thermal diffusivity of air [m^2/s]
A_{spec}	specific transfer area [m^2/m^3]
c	vapour concentration [kg/m^3]
c_p	heat capacity [J/kg K]
D	diffusion coefficient [m^2/s]
k	wave number [1/m]
L	length [m]
r	heat of evaporation [J/kg]
s	relaxation rate [1/s]
t	time [s]
T	temperature [K]
u	velocity [m/s]
x	spatial co-ordinate [m]
α	heat transfer coefficient [W/m^2 K]
β	mass transfer coefficient [m/s]
ϵ	porosity of flowerbed
λ	heat conductivity [W/m K]
ρ	mass density [kg/m^3]

Symbols of LB scheme

c_i	propagation speeds
D	diffusion coefficient
g_i	number of lattice gas particles
h_i	number of heat particles
j	particle flux of
K	wave number
N	number of lattice sites
Pe^*	grid Peclet number
U	Courant number
v_i	distribution of vapour lattice gas particles
ϕ	transfer rate
Φ	transfer operator
μ	Knudsen number
ρ	density of lattice gas particles
ω	relaxation rate
Ω	collision operator

Super- and subscripts

a	air
eq	equilibrium
g	generic lattice gas
h	heat particles in air
i	state index
(n)	nth order perturbation
p	product
q	stagnant heat particles
sat	saturated
v	vapour particles
0	ambient condition
1	initial condition

In most transport packaging systems the heat and mass transfer is dominated by a convection–diffusion process. The numerical solution of this phenomenon is a complex problem. Thus, in order to obtain a reliable solution with Finite Element or Finite Difference schemes, advanced mathematical techniques are required [2,6].

An alternative numerical solution method of the convection–diffusion problem, requiring little advanced mathematics, is the recently developed technique of the Lattice Boltzmann (LB) scheme [8,14]. LB schemes simulate physical transport phenomena with quasi particles, populating a regular lattice. The dynamics of these so-called lattice gas particles are stripped to the barest essentials: the particles move across the lattice along links connecting neighbouring lattice sites, and upon arrival at a lattice site the particles undergo collisions. In order to simulate physical phenomena the collisions must satisfy appropriate conservation laws and the lattice must exhibit certain symmetries. Using simple collision rules, various complex phenomena have been modelled successfully, such as Navier–Stokes flow [8,9], convection–diffusion [10], reaction diffusion [11], and natural convection [12].

The straightforward principles of the LB scheme give it some attractive properties, relevant to our applications. These properties are: (1) it is applicable to a large class of physical and biological phenomena; (2) it can easily handle complex geometry and boundary conditions, with simple and strictly local rules; and (3) its implementation on the computer is relatively straightforward. Given these properties, the LB scheme appears to be a suitable choice for the general framework for the model-based approach of the heat and mass transfer in packaging systems.

In this paper, a LB scheme modelling the heat and water vapour transfer during the cooling of packed cut flowers is presented. These processes can be described with one-dimensional convection–diffusion equations with source terms representing the convective heat and mass transfer between product and airflow [13]. We use this problem as a case study for the investigation of the capabilities and the practical usefulness of the LB scheme towards our objectives.

Before treating the full problem of cooling packed cut flowers, a reduced problem is considered, which involves only heat transfer. The performance of the LB scheme is analysed both mathematically and numeri-

cally. A one-dimensional convection–diffusion LB scheme will be derived from an existing 2-D LB scheme [10], which considers convection–diffusion in conjunction with Navier–Stokes flow. For the 1-D convection–diffusion scheme we expect similar performance as the scheme of Flekkoy [10], i.e. the scheme has good (second order) accuracy and little numerical diffusion even at moderately high grid Peclet numbers and high Courant numbers.

For the modelling of heat transfer between flowers and airflow, the 1-D convection–diffusion scheme is extended with a source term. The consistency of the extended scheme is analysed mathematically with the Chapman–Enskog procedure, a standard tool in kinetic theory [16]. Subsequently, the accuracy of the extended scheme is analysed by solving a problem, involving heat transfer between flower and airflow, which has an exact solution.

After checking the consistency of the scheme with a convection–diffusion equation having a heat transfer source term, the scheme is extended with the water vapour transfer processes in the packed bed of flowers. With this final scheme simulations of the cooling behaviour of packaged cut flowers are performed and compared with data of cooling experiments. From the comparison between numerical simulation and experiment and from the previous numerical and mathematical analysis, conclusions are drawn for the usefulness of the LB scheme as a modelling tool for physical transport phenomena in packaging systems.

2. Convection–diffusion scheme with heat transfer

The reduced problem, considering only the heat transfer in flower packages, is mathematically described by the following set of partial differential equations [13]:

$$\partial_t T_a + u\partial_x T_a = s_a(T_p - T_a) + a\partial_x^2 T_a, \tag{1}$$

$$\partial_t T_p = s_p(T_a - T_p). \tag{2}$$

Here T_a is the temperature of the air flowing with velocity u and T_p is the temperature of the cut flowers. The time and spatial derivatives are denoted by ∂_t and ∂_x, respectively. The relaxation constants s_a and s_p are determined by the heat resistance of the boundary layer between the flowers and the surrounding air. The thermal diffusivity of air is a.

Before presenting the LB scheme for the solution of the reduced problem Eqs. (1) and (2), the general principles and the numerical properties of the convection–diffusion Lattice Boltzmann scheme are briefly described.

2.1. 1-D convection–diffusion scheme

LB schemes essentially describe the evolution of the particle distribution of a lattice gas, whose density represents the physical quantities to be modelled, such as temperature. The particle distribution functions $g_i(\mathbf{x}, t)$ denote the number of particles propagating with velocity $\mathbf{c}_i$ along the lattice link $\Delta\mathbf{x}_i = \mathbf{c}_i\Delta t$ connecting nearest neighbours. The particle number density is obtained after summing g_i over all states, i.e. $\rho_g(\mathbf{x}, t) = \Sigma_i g_i(\mathbf{x}, t)$. The particle number density can be related to macroscopic observable quantities, such as temperature, concentrations etc. The particle distribution evolves as particles propagate to neighbouring lattice sites, where they collide with other particles. Thus, the evolution of g_i can be described with a collision step followed by a propagation step:

$$g_i(\mathbf{x}, t)' = g_i(\mathbf{x}, t) + \omega_g[g_i^{eq}(\mathbf{x}, t) - g_i(\mathbf{x}, t)], \tag{3}$$

$$g_i(\mathbf{x} + \Delta\mathbf{x}_i, t + \Delta t) = g_i(\mathbf{x}, t)'. \tag{4}$$

The collisions are modelled as a relaxation towards an equilibrium distribution g_i^{eq}, as is common practice in classical kinetic theory [16]. Combining Eqs. (3) and (4) one obtains the Lattice Boltzmann equation, which can be regarded as a discretisation of the classical Boltzmann equation. ω_g controls the relaxation towards equilibrium and is related to physical transport coefficients like diffusivity and viscosity.

For convection–diffusion the equilibrium distribution has the following form [10]:

$$g_i^{eq}(\mathbf{x}, t) = w_i\rho_g(x, t)\left[1 + \frac{\mathbf{c}_i\mathbf{u}}{c_s^2}\right], \tag{5}$$

with the weight factor w_i defined by

$$w_i = \frac{c_s^2}{2c_i^2}, \tag{6}$$

and the 'speed of sound' c_s defined by

$$c_s^2 = \sum_i \frac{1}{2c_i^2}. \tag{7}$$

For convection–diffusion the parameter c_s has no physical meaning. In LB schemes modelling Navier–Stokes flow, it does have the meaning of the speed of sound. The value of the speed of sound of the lattice gas is dependent on the type of lattice applied (i.e. the set of allowed particle velocities $\{\mathbf{c}_i\}$).

The expression for the equilibrium distribution for the convection–diffusion scheme follows naturally from the constraints:

$$\sum_i g_i^{\mathrm{eq}}(\mathbf{x},\, t) = \rho_{\mathrm{g}}(\mathbf{x},\, t), \tag{8}$$

$$\sum_i \mathbf{c}_i g_i^{\mathrm{eq}}(\mathbf{x},\, t) = \rho_{\mathrm{g}}(\mathbf{x},\, t)\mathbf{u}. \tag{9}$$

Having the appropriate equilibrium distribution Eq. (5), the number density $\rho_{\mathrm{g}}(\mathbf{x},\, t)$ will evolve according to a convection–diffusion equation, as is mathematically derived by Flekkoy [10]. The diffusion coefficient is related to the relaxation parameter ω_{g}. In the limit of low Courant numbers ($U = u\Delta t/\Delta x$) the diffusion coefficient is equal to

$$D = c_{\mathrm{s}}^2\left(\frac{1}{\omega_{\mathrm{g}}} - \frac{1}{2}\right)\Delta t. \tag{10}$$

At higher Courant numbers the diffusion coefficient is also velocity dependent. In the Appendix the equation for the velocity dependent diffusion coefficient is derived.

For the problem, covered in this paper, one-dimensional convection–diffusion is considered. The configuration of the lattice is readily derived from Eqs. (8) and (9). The 1-D lattice is populated with particles propagating either to the left or to the right, i.e. $c_i = \pm\Delta x/\Delta t$, with $i = 1,\, 2$. The weight factors are $w_i = \frac{1}{2}$ and the speed of sound is $c_{\mathrm{s}} = \Delta x/\Delta t$.

2.2. 1-D convection–diffusion scheme with source terms

The consistency and accuracy of the 1-D convection–diffusion LB scheme extended with a source term, describing the heat transfer between packed flowers and the airflow through the bed, is investigated below.

In this extended LB scheme the amount of heat, in the air in the packed bed of flowers, is modelled by the lattice gas distribution function h_i. The density of this gas is proportional to the air temperature: $\rho_{\mathrm{h}} = \Sigma_i h_i = T_{\mathrm{a}}$. The heat of the flowers is modelled by stagnant particles with density ρ_{q}, which is proportional to the product temperature: $\rho_{\mathrm{q}} = T_{\mathrm{p}}$.

The extended LB scheme reads as follows:

$$h_i(x + \mathbf{c}_i\Delta t,\, t + \Delta t) - h_i(x,\, t) = \omega_{\mathrm{h}}[h_i^{\mathrm{eq}}(x,\, t) - h_i(x,\, t)] + \Phi_i^{\mathrm{h}}(x,\, t), \tag{11}$$

$$\rho_{\mathrm{q}}(x,\, t + \Delta t) - \rho_{\mathrm{q}}(x,\, t) = \Phi^{\mathrm{q}}(x,\, t), \tag{12}$$

with the equilibrium distribution defined by Eq. (5) and the source term defined by:

$$\Phi_i^{\mathrm{h}}(x,\, t) = \frac{\phi_{\mathrm{h}}}{2}[\rho_{\mathrm{q}}(x,\, t) - \rho_{\mathrm{h}}(x,\, t)], \tag{13}$$

$$\Phi^{\mathrm{q}}(x,\, t) = \phi_{\mathrm{q}}[\rho_{\mathrm{h}}(x,\, t) - \rho_{\mathrm{q}}(x,\, t)]. \tag{14}$$

Since previous LB schemes have not addressed heat transfer processes, the collision operator Φ_i^{h} has to be constructed using physical arguments. We have postulated, that Φ_i^{h} is a weighted function of the transferred heat, with weights equal to $w_i = \frac{1}{2}$. The heat of the flowers is modelled with stagnant particles ($c_i = 0$), whose density, ρ_{q}, evolves according to the first order discretisation of Eq. (2).

In order to determine the consistency of our LB scheme with the physical phenomena considered, and to establish the relationships between the physical parameters and the model parameters, we have performed the Chapman–Enskog procedure [8]. This is a standard technique in kinetic theory, where it is used to derive the macroscopic transport equations from the classical Boltzmann equation [16]. This technique can equally well be applied to the Lattice Boltzmann equation [10,11]. In the Appendix we show by using the Chapman–Enskog procedure, that the LB scheme models Eqs. (1) and (2) with second order accuracy. Furthermore, the following relations between the model parameters of the LB scheme and the physical parameters are obtained:

$$a = c_{\mathrm{s}}^2\left(\frac{1}{\omega_{\mathrm{h}}} - \frac{1}{2}\right)\Delta t; \quad s_{\mathrm{a}} = \frac{\phi_{\mathrm{h}}}{\Delta t}; \quad s_{\mathrm{p}} = \frac{\phi_{\mathrm{q}}}{\Delta t}. \tag{15}$$

The accuracy of the LB scheme is studied numerically by comparing the computational results with an exact solution, which holds for the problem of a semi-infinite packed bed with a periodically varying heat source at the origin. The temperature of the incoming airflow is giving by

$$T_{\mathrm{a}}(x = 0,\, t) = T_0 + \tilde{T}_{\mathrm{a}}\ \cos(st). \tag{16}$$

The exact periodic stationary solution is obtained by substituting

$$T_{\mathrm{a}}(x,\, t) = T_0 + \tilde{T}_{\mathrm{a}}\ \exp(-kx + ist), \tag{17}$$

$$T_{\mathrm{p}}(x,\, t) = T_0 + \tilde{T}_{\mathrm{p}}\ \exp(-kx + ist), \tag{18}$$

into Eqs. (1) and (2). The value of the wave number k is obtained by solving the following equation:

$$-ak^2 + uk + s_{\mathrm{a}} - is + \frac{s_{\mathrm{a}}s_{\mathrm{p}}}{s_{\mathrm{p}} - is} = 0. \tag{19}$$

Injecting an appropriate amount of particles at the origin varies the temperature of the heat source, such that the following condition is satisfied:

$$\sum_i h_i(x = 0,\, t) = T_{\mathrm{a}}(x = 0,\, t). \tag{20}$$

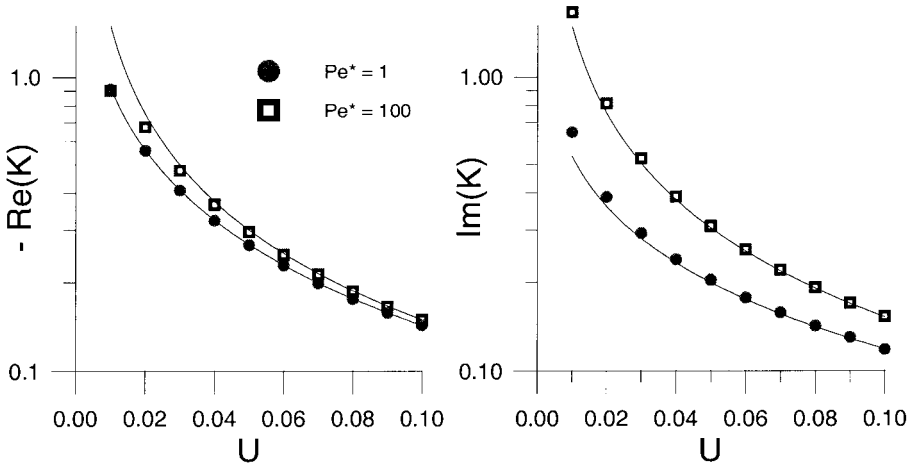

Fig. 1. Comparison of the solution of LB scheme (symbols) with the exact solution (lines) of the problem of a semi-infinite packed bed with periodically varying heat source at the origin. Shown is the value of the wave vector K of the exact solution as a function of the Courant number U for the grid Peclet number $Pe^*=1$ and 100.

Calculations are performed with the grid Peclet number $Pe^*=u\Delta x/a = 1$ and $Pe^*=100$, for values of the Courant number $U=u\Delta t/\Delta x$ in the range of $0.01 \leq U \leq 0.1$, and for $s_a=0.3\ s^{-1}$ and $s_p=0.003\ s^{-1}$, which are typical values for packed beds of agricultural products. In our simulations we have set $s=s_p$, such that large values for the wave number k can be obtained. From the simulation results the dimensionless complex wave number $K=k\Delta x$ is computed using non-linear regression. These values have been compared with the root of Eq. (19), as is shown in Fig. 1.

For the range of $Re(K) > -0.4$ we have obtained accurate results, the differences between the estimated and the exact values of K are within 2% for both $Pe^*=1$ and $Pe^*=100$. If the ratio of the macroscopic length scale k^{-1} and the lattice spacing Δx approaches unity ($\mu \approx K \rightarrow 1$), the LB scheme looses accuracy, especially in the case of high Peclet numbers. This is not unexpected considering that the Chapman–Enskog expansion is valid only in the range of the Knudsen number $\mu < 1$. As such, steep gradients can not be resolved accurately by the LB scheme. However, this is a property shared with many other numerical schemes.

3. Cooling of packed cut flowers

After checking the consistency of our LB scheme, an extended scheme for the problem of cooling cut flowers has been developed. Packed cut flowers are cooled by forcing cold air through the vent holes in the package and subsequently through the bed of flowers, as is shown in Fig. 2. In this case study, the packaging considered is in the middle of a large stack, with adjacent packages at all sides. All packages in the stack are ventilated with an equal amount of airflow. Consequently, the cooling process of flowers in the box in the middle of the stack can be treated as a one-dimensional problem. Further assumptions are:

1. The flower bed is a porous medium with homogeneous porosity, resulting in a uniform flow field through the bed.
2. The heat conduction of the solid phase of the flowerbed is negligible, due to limited contact between the individual flowers.
3. The heat production by respiration is negligible.
4. The flower plants maintain a saturated vapour pressure in their tissue.

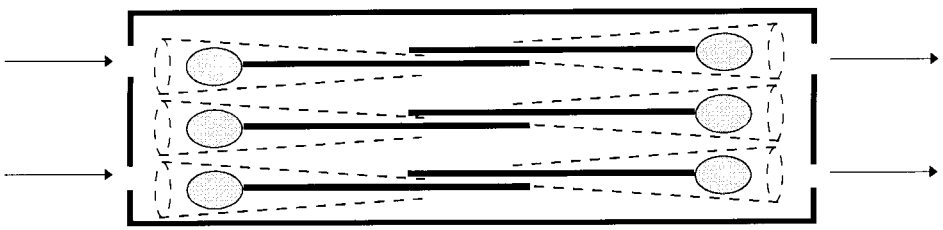

Fig. 2. Schematic diagram of packaging for cut flowers. The flowers face either side of the box and are wrapped in foil, indicated with dashed lines.

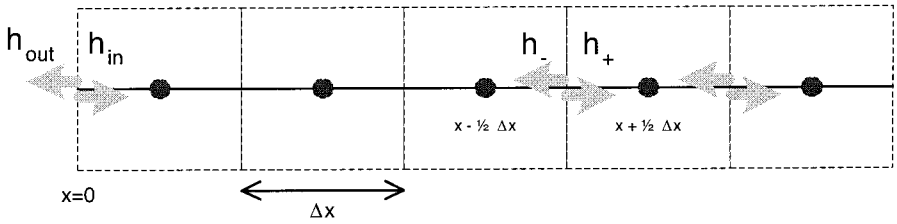

Fig. 3. Particle flux j_h at the boundary of the Wigner–Seitz cell (dashed lines), defined as $j_h(x) = c[h_+(x + \frac{1}{2}\Delta x) - h_-(x - \frac{1}{2}\Delta x)]$. At the boundary $x = 0$ the particle flux is defined as $j_h(0) = c[h_{in} - h_{out}]$.

5. The saturated vapour pressure is a function of the flower temperature.
6. There is vapour transfer between product and surrounding air, which is proportional to the vapour deficit between the plant tissue and the air.

Applying the above assumptions the heat and vapour transfer can be described by the following equations [2,5]:

$$\partial_t T_a + u\partial_x T_a = a\partial_x^2 T_a + s_a(T_p - T_a), \tag{21}$$

$$\partial_t T_p = s_p(T_a - T_p) + s_w(c_a - c_a^{sat}), \tag{22}$$

$$\partial_t c_a + u\partial_x c_a = D\partial_x^2 c_a + s_v(c_a^{sat} - c_a). \tag{23}$$

These equations are obtained by extending Eqs. (1) and (2) with a convection–diffusion equation governing the water vapour transport in air. The source term in Eq. (23) accounts for the evaporation of water from the cell tissue of the flowers. The heat of evaporation is extracted from the heat of the flowers and is accounted by the extra source term in Eq. (21).

The relaxation constants:

$$s_a = \frac{\alpha A_{spec}}{\rho_a c_{p_a} \epsilon}, \quad s_p = \frac{\alpha A_{spec}}{\rho_p c_{p_p}(1-\epsilon)}, \quad s_w = \frac{r\beta A_{spec}}{\rho_p c_{p_p}(1-\epsilon)}, \quad s_v = \frac{\beta A_{spec}}{\epsilon}, \tag{24}$$

are determined by the heat and mass transfer coefficient of the flower plants tissue and the boundary layer between the flower and the surrounding air flow.

The description of the physical system, Eqs. (21)–(23), is completed with the initial and boundary conditions at the in flow ($x = 0$) and out flow ($x = L$) boundaries of the bed of product:

$$T_a = T_p = T_1, \quad c_a = c_a^{sat}(T_1), \quad \text{for all } x > 0, \text{ at } t = 0; \tag{25}$$

$$T_a = T_0, \quad c_a = c_{a0}, \quad \text{for all } t, \text{ at } x = 0, \tag{26}$$

$$\partial_x T_a = \partial_x c_a = 0, \quad \text{for all } t, \text{ at } x = L. \tag{27}$$

The modelling of the vapour transfer during cooling requires that another lattice gas with distribution function v_i is introduced in the LB scheme. The density of this lattice gas represents the vapour density $\Sigma_i v_i = \rho_v$. The particle distribution v_i evolves according to a LB equation similar to Eq. (11). The density of the vapour particles in the flowers is maintained at the saturation vapour pressure ρ_v^{sat} and therefore it is not modelled explicitly. The complete extended LB scheme describing the cooling of flowers is given below:

$$h_i(x + \Delta x_i, t + \Delta t) - h_i(x, t) = \Omega_i^h(x, t) + \Phi_i^h(x, t), \tag{28}$$

$$v_i(x + \Delta x_i, t + \Delta t) - v_i(x, t) = \Omega_i^v(x, t) + \Phi_i^v(x, t), \tag{29}$$

$$\rho_q(x, t + \Delta t) - \rho_q(x, t) = \Phi^q(x, t) + \Phi^w(x, t). \tag{30}$$

The collision operator,

$$\Omega_i^v(x, t) = \omega_v[v_i^{eq}(x, t) - v_i(x, t)], \tag{31}$$

describes the transport of vapour in the air flow and the transfer operators

$$\Phi_i^v(x, t) = w_i\phi_v[\rho_v^{sat}(x, t) - \rho_v(x, t)], \tag{32}$$

$$\Phi^w(x, t) = \phi_w[\rho_v(x, t) - \rho_v^{sat}(x, t)], \tag{33}$$

describe the vapour transport by evaporation from flowers to air. For the definition of the other operators we refer to the previous section.

The relations between the parameters in the LB scheme and the physical parameters are given by:

$$D = c_s^2\left(\frac{1}{\omega_v} - \frac{1}{2}\right)\Delta t; \quad s_v = \frac{\phi_v}{\Delta t}; \quad s_w = \frac{\phi_w}{\Delta t}. \tag{34}$$

3.1. Initial and boundary conditions

The initial particle distributions are set equal to the equilibrium distributions corresponding with the initial temperature $\rho_{h1} = T_1$ and vapour concentration $\rho_{v1} = c_a^{sat}(T_1)$, i.e.

$$h_i(x,\, t=0) = h_i^{eq}(\rho_{h0}), \tag{35}$$

$$v_i(x,\, t=0) = v_i^{eq}(\rho_{v0}), \tag{36}$$

$$\rho_q(x,\, t=0) = \rho_{h0}. \tag{37}$$

In LB schemes it is convenient and natural to prescribe the boundary conditions in terms of the particle fluxes, j_h and j_v, crossing the boundaries of the lattice cells [19]. These boundaries are midway between the links connecting adjacent lattice sites and bound the Wigner–Seitz cell, which is the primitive lattice cell with the lattice site in the centre [20], as shown in Fig. 3. The particle flux crossing the boundaries of the lattice cell are equal to the number of particles propagating to the right minus the number of particles propagating to the left, multiplied by their propagation speed $|\, c_i \,| = c = \Delta x/\Delta t$, i.e.

$$j_h(x,\, t) = \sum_i c_i h_i\left(x + \frac{1}{2}\Delta x_i,\, t\right), \tag{38}$$

$$j_v(x,\, t) = \sum_i c_i v_i\left(x + \frac{1}{2}\Delta x_i,\, t\right). \tag{39}$$

Such a definition can also be stated for the particle fluxes leaving the computational domain. Hence, the fluxes at the boundaries of the lattice are proportional to the number of particles leaving the lattice minus the number of particles injected into the lattice.

For the determination of the values of the particle fluxes leaving the lattice, we split the particle flux into a equilibrium part and a non-equilibrium part: $j_h = j_h^{eq} + j_h^{neq}$. The equilibrium particle flux is due to the externally applied velocity field: $j_h^{eq} = \rho_h u$. The non-equilibrium particle flux is due to gradients in the number density and follows Fouriers law, e.g. Ficks law. For the computation of the non-equilibrium particle flux at the inlet we use a first order approximation of Fouriers law and Ficks law. At the outlet ($x = L$) the gradients are zero according to the boundary conditions Eq. (27). Hence, the boundary conditions, stated as prescription of the particle fluxes leaving the lattice, are given by:

$$j_h(x=0,\, t) = \frac{a}{\frac{1}{2}\Delta x}\left[\rho_h\left(x = \frac{1}{2}\Delta x,\, t\right) - \rho_{h1}\right] + \rho_{h1}u, \tag{40}$$

$$j_v(x=0,\, t) = \frac{D}{\frac{1}{2}\Delta x}\left[\rho_v\left(x = \frac{1}{2}\Delta x,\, t\right) - \rho_{v1}\right] + \rho_{v1}u, \tag{41}$$

$$j_h(x=L,\, t) = \rho_h\left(x = L - \frac{1}{2}\Delta x,\, t\right)u, \tag{42}$$

$$j_v(x=L,\, t) = \rho_v\left(x = L - \frac{1}{2}\Delta x,\, t\right)u. \tag{43}$$

Here, ρ_{h1} and ρ_{v1} are the densities of heat and water vapour particles at the inlet, respectively.

As the boundaries of the computation domain coincide with the boundaries of the lattice cells, they are displaced half a lattice spacing from the nearest lattice site. Therefore, the location of the lattice sites are labelled as $x = (\frac{1}{2} + n)\Delta x$, with $0 \le n \le N-1$ and $N = L/\Delta x$ the number of lattice sites.

3.2. Experiments

Simulation results, obtained by the LB scheme, are compared with data from cooling experiments performed with irises, cultivar Blue Magic. Irises are chosen since the flowerbed has a high degree of homogeneity in porosity and mass density. Due to the homogeneity of the porosity the airflow inside the flowerbed will be quite uniform.

The irises are packed in a commercially used box, made from corrugated board and measuring $1.20 \times 0.45 \times 0.30$ m. The thickness of the corrugated board is 4 mm at the top and bottom, and 8 mm at the sides. At both ends of the box there are two vent holes (diameter = 6 cm). The flower buds face either ends of the box, as shown in Fig. 2. The box contains 18 bunches consisting of 50 irises each, having a total mass 35.5 kg. Each bunch is wrapped in polypropylene foil, which is impermeable to airflow and vapour transport. The foil wrapping is open at both ends of the bunch. As the bunch stacking in the box is very tight, we assume that the total flow is going through the bunches. The length of the flowerbed is 1.00 m, leaving two headspaces of 0.10 m at both ends of the box.

The temperature of the flowers is monitored with copper-constantane thermocouples, which are inserted either in the back of the flower bud or the end of the stems. In total 20 thermocouples, more or less uni-

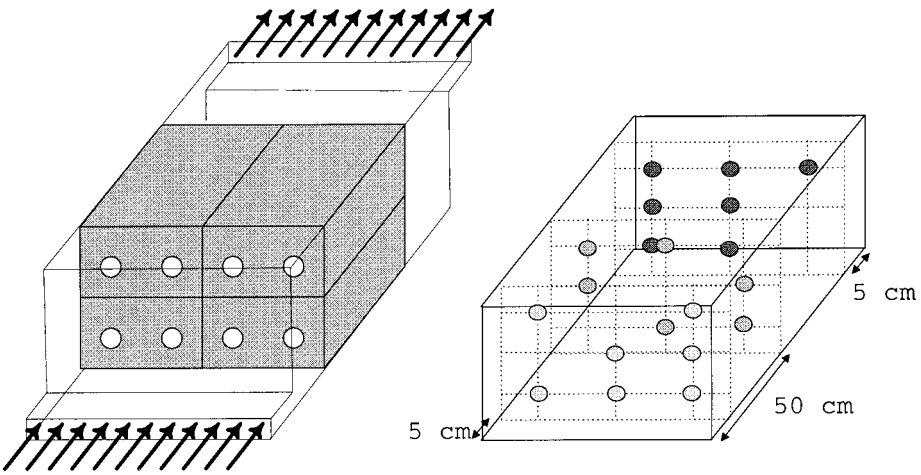

Fig. 4. Experimental setup for monitoring the cooling of packaged flowers. On the left the container with four packagings is drawn. On the right the locations of the thermocouples are indicated.

formly distributed over the front, middle and the back cross section, are used. The positions of these cross sections and the positions of the thermocouples within the cross section are indicated in Fig. 4.

The experiment is performed with cooling conditions as occur during road transport. Prior to the cooling, the packed flowers are stored for 24 h in a climate room controlled at 19°C, giving the flowers a uniform initial temperature. After this pre-treatment the box with flowers is put in an insulated container. Also, 3 other identical boxes, which are filled with synthetic material (artificial lemons, partially filled with water), are placed in the container. The weight and consequently, the heat capacity of the artificial lemons are about equal to that of the flowers. The airflow resistance of the artificial is also comparable to that of the packed bed of irises. Due to the similarity in thermal and aerodynamic properties, and the low thermal conductivity of the corrugated board, we assume that there is no heat flow from one box to another. Hence, the cooling of the packed irises is assumed to be a 1-D problem.

Subsequently, the container with the boxes is stored in another climate room, which is controlled at a temperature of 3°C and a relative humidity of 90%. The temperature and the relative humidity of the air at the inlet are measured with a Vaisailla temperature and R.H.-sensor. With a fan system, the cold air from the room is forced into the container, flows through the boxes and exists again in the climate room. The container and the flow of air are indicated in Fig. 4. At the outlet the air flow velocity is measured with a hot wire anemometer. Due to the high turbulence and the division of the airflow over four boxes, the velocity field inside the box with flowers can not be obtained accurately. The fan system is regulated such that airflow velocity inside the flower box is in the range of 5–10 cm/s, which is the range of airflow inside packages during road transport.

The readings of the thermocouples and the Vaisalla sensor are recorded with a data logger, sampling at a 2 min interval. An average reading of the thermocouples over the last hour of the pre-treatment shows that the initial flower temperature is 18.8 ± 0.3°C. The inaccuracy in the initial flower temperature is mainly due to the non-uniformity of the temperature distribution. The average reading during cooling shows that the inlet air temperature is 2.8 ± 0.1°C and a relative humidity of $90 \pm 5\%$.

The accuracy of the readings of the flower temperature during cooling is determined by averaging the values measured at the end of the cooling during which a steady state is obtained. Averaging 20 values of a single thermocouple shows a standard deviation of 0.014°C, and after averaging 20 readings from all thermocouples in the back cross section one obtains the average value of the final flower temperature of 2.4°C with a standard deviation of 0.14°C. The low value of the standard deviation indicated a rather uniform temperature distribution in the back cross section. Other cross sections show similar standard deviations, and thereby substantiating the hypothesis that the cooling of the packed irises in this experiment is a 1-D phenomenon.

It is worthy of noting that the final flower temperature, 2.4°C, is lower than the inlet air temperature, 2.8°C. This effect cannot be explained by an inaccuracy in the measurement of the temperatures. In fact, this difference is caused by the evaporation of water from the flower plant, which extracts heat from the flower and hence lowers the flower temperature below the air temperature [13].

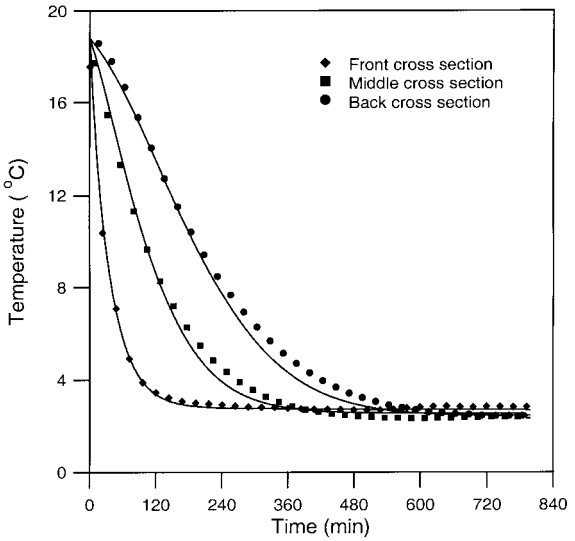

Fig. 5. Comparison of experiment (symbols) with simulation data from the LB scheme (lines). Shown is the change in time of the average flower temperature in three cross sections of the flower bed during cooling.

3.3. Simulation

With the Lattice Boltzmann scheme the cooling of packed irises, as recorded in the previously described experiment, is simulated. The numerical results will be compared with the averaged flower temperatures in the three cross sections, which are indicated in Fig. 4.

The simulation with the LB scheme is performed with a lattice with 20 grid points and Courant number of $U = u\Delta t/\Delta x = 0.1$, and a grid Peclet number $Pe^* \approx 250$. With the value of $U = 0.1$ we have a error of the diffusion coefficient which is less than 1%, see Eq. (53).

The physical properties of the flowers are approximately equal to those of water [1]. The initial flower temperature and the inlet air temperature and relative humidity are taken equal to the values measured during the experiment. Three remaining parameters, αA_{spec}, βA_{spec} and u, are difficult to determine, due to the intricate geometry of the individual flowers and the inaccuracy in the air velocity measurement. Thus, they are estimated from the experimental data by trial simulations.

We have adjusted the yet undetermined parameters u, αA_{spec} and βA_{spec} until the sum of squared residuals is minimised. In Fig. 5 the simulation results, computed with the final parameter set $u = 0.067$ m/s, $\alpha A_{\text{spec}} = 443$ W/m^3 K and $\beta A_{\text{spec}} = 0.056$ s^{-1}, can be seen.

Fig. 5 shows that the simulation results correlate well with the experimental data. The simulation indeed shows that in the steady state at the end of cooling, the average flower temperature (in the middle and back cross section), $T_p = 2.4$°C, is lower than the incoming air, $T_0 = 2.8$°C. This phenomenon can indeed be explained by the extra cooling effect of the evaporation of water from the flowers.

4. Conclusions

For the analysis of the heat and mass transfer in packaging systems with cut flowers, a 1-D convection–diffusion Lattice Boltzmann scheme has been constructed. The consistency and accuracy of this scheme is checked by performing benchmark problems and by theoretical analysis.

In the first instance, a convection–diffusion scheme extended with source terms to represent the heat transfer from packed flowers to the airflow, is analysed. With the help of mathematical analysis of the Chapman–Enskog procedure and of numerical analysis, LB schemes have shown to accurately simulate the phenomena described with convection–diffusion and simultaneous heat transfer, e.g. Eqs. (1) and (2). Accurate agreement with exact solutions is found for both low and high grid Peclet numbers Pe^*, with the restriction that the gradient should not be too steep. Since large gradients in temperature or vapour density in systems of packed agricultural products seldom occur in practice, the limitation of the LB scheme is not very restrictive for our applications.

Finally, the extended LB scheme is applied to the problem of cooling packaged cut flowers. Next to heat flow phenomena, the scheme also describes the vapour flow phenomena. The scheme is able to simulate cooling experiments with packed irises with reasonable accuracy. The simulation is performed with high grid Peclet numbers, i.e. $Pe^* \approx 250$ and with a small amount of resources (lattice of 20 grid points).

Based on the results of this study, it is concluded that the Lattice Boltzmann scheme is suitable as a generic modelling technique for the simulation of physical processes in packages of agricultural products. In future research the scheme will be extended to higher dimensions and with other physical phenomena, such as natural convection.

Appendix. Chapman–Enskog procedure

The application of the Chapman–Enskog procedure to a Lattice Boltzmann equation reveals its macroscopic behaviour, as triggered by small departures of the equilibrium distribution [8].

In the Chapman–Enskog expansion the particle distribution function h_i is expanded as a power series of

the Knudsen number μ, which is the ratio of the mean free path and the macroscopic length scale: $\mu \sim \Delta x \partial_x \rho_h / \rho_h$. The expansion of h_i around its equilibrium distribution is:

$$h_i = h_i^{eq} + \mu h_i^{(1)} + \mu^2 h_i^{(2)} + \cdots \tag{44}$$

It must be noted that the Chapman–Enskog expansion is made under the assumption that $\mu < 1$.

Also space and time derivatives of h_i are expanded as series in powers of μ. The Chapman–Enskog procedure introduces two time scales, a fast time scale, t_1, associated with convective (inertial) processes and a slow time scale, t_2, associated with dissipative processes, i.e. heat conduction. By the introduction of the two time scales into the time derivative and the substitution $x_1 = \mu x / \Delta x$ in the spatial derivative the following is obtained:

$$\Delta x \partial_x h_i = \mu \partial_{x_1} h_i \tag{45}$$

$$\Delta t \partial_t h_i = \mu \partial_{t_1} h_i + \mu^2 \partial_{t_2} h_i \tag{46}$$

As the heat transfer process, modelled by Φ_i^h, is also a dissipative process it can be assumed that it also scales as μ^2: $\Phi_i^h = w_i \mu^2 \tilde{\phi}_h (\rho_h - \rho_q)$.

After substitution of the expansions Eqs. (44)–(46) into the LB scheme, Eqs. (11)–(14), performing a Taylor expansion of $h_i(x + \Delta x_i, t + \Delta t)$, and collecting terms of equal order in μ, one obtains the following hierarchy of equations:

$$-\omega_h h_i^{(1)} = (\partial_{t_1} + e_i \partial_{x_1}) h_i^{eq} \tag{47}$$

$$-\omega_h h_i^{(2)} = (\partial_{t_1} + e_i \partial_{x_1})^2 h_i^{eq} + (\partial_{t_1} + e_i \partial_{x_1}) h_i^{(1)} + \partial_{t_2} h_i^{eq} \tag{48}$$

Here, $e_i = c_i \Delta t / \Delta x$.

After summing Eq. (47) over all states and using $\Sigma_i h_i^{(n)} = 0$, one obtains the evolution of the density ρ_h for short time scales, with $U = u \Delta t / \Delta x$ the Courant number:

$$\partial_{t_1} \rho_h + U \partial_{x_1} \rho_h = 0. \tag{49}$$

Observe, at short time scales the density evolves according to the continuity equation, as must be expected.

Substitution of Eq. (47) in Eq. (48) and summing over all states, one obtains the contribution of the long time scale to the evolution of ρ_h:

$$\partial_{t_2} \rho_h = \left(\frac{1}{\omega_h} - \frac{1}{2} \right) (1 - U^2) \partial_{x_1}^2 \rho_h + \tilde{\phi}_h (\rho_q - \rho_h). \tag{50}$$

The PDE describing the evolution of ρ_q follows directly from the expansion of Eq. (14). The complete set of PDE's, Eqs. (1) and (2), is recovered when the contributions of both times scales, t_1 and t_2, are added:

$$\partial_t \rho_h + u \partial_x \rho_h = D_h \partial_x^2 \rho_h + \frac{\phi_h}{\Delta t} (\rho_q - \rho_h) \tag{51}$$

$$\partial_t \rho_q = \frac{\phi_q}{\Delta t} (\rho_h - \rho_q). \tag{52}$$

For the diffusion coefficient, it follows that:

$$D_h = \frac{\Delta x^2}{\Delta t} \left(\frac{1}{\omega_h} - \frac{1}{2} \right) (1 - U^2). \tag{53}$$

The velocity dependent term $(1-U^2)$ is in agreement with classical kinetic theory [16]. This term arises in the regime of compressible flow. The velocity dependence is negligible in the limit of low velocities, which is the incompressible flow regime where Lattice Boltzmann schemes normally operate. However, recently it is shown, that the velocity dependent term can be eliminated, if rest particles with $c_i = 0$ are introduced and if quadratic terms in U are incorporated in the equilibrium distribution [22].

References

[1] G. van Beek, H.F.Th Meffert, Cooling of horticultural product with heat and mass transfer by diffusion, in: E. Thorne (Ed.), Developments in Food Preservation, vol. 1, Applied Science Publishers, London, 1981, pp. 39–92.

[2] K.J. Beukema, Heat and mass transfer during cooling and storage of agricultural products as influenced by natural convection, Ph.D. thesis, Agricultural University, Wageningen, The Netherlands, 1980.

[3] R.G.M. van der Sman, R.G. Evelo, E.C. Wilkinson, W.G. van Doorn, Quality loss in packed rose flowers due to Botrytis cinerea as related to temperature regimes and packaging design, Postharvest Biol. and Techn. 7 (1996) 341–350.

[4] C.D. Baird, J.J. Gaffney, A numerical procedure for calculating heat transfer in bulk loads of fruits or vegetables, Trans. ASHRAE 82 (2) (1982) 525–540.

[5] F.W. Bakker-Arkema, W.G. Bickert, R.J. Patterson, Simultaneous heat and mass transfer during the cooling of a deep bed of biological products under varying inlet air conditions, J. Agr. Eng. Research 12 (4) (1967) 297–307.

[6] K.K. Khankari, S.V. Patankar, R.V. Morey, A mathematical model for natural convection moisture migration in stored grain, ASEA-paper 93-6017, 1–29, 1993.

[7] G. Comini, G. Cortella, O. Saro, Finite element analysis of coupled conduction and convection in refrigerated transport, Int. J. Refrig. 18 (2) (1995) 123–131.

[8] U. Frisch, D. d'Humieres, D.B. Hasslacher, Y. Pomeau,

J.P. Rivet, Lattice gas hydrodynamics in two and three dimensions, Complex Systems 1 (1987) 649–707.

[9] J.M.V.A. Koelman, A simple Lattice Boltzmann scheme for Navier–Stokes fluid flow, Europhys. Lett. 15 (6) (1991) 603–607.

[10] E.G. Flekkoy, Lattice BGK model for miscible fluids, Phys. Rev. E 47 (1993) 4247.

[11] S. Ponce-Dawson, S. Chen, G.D. Doolen, Lattice Boltzmann computations for reaction–diffusion equations, J. Chem. Phys. 98 (2) (1993) 1514–1523.

[12] J.G.M. Eggels, J.A. Somers, Numerical simulation of free convective flow using the lattice-Boltzmann scheme, Int. J. Heat and Fluid Flow 15 (1995) 357–364.

[13] H. Wang, C. Ceton, S. Touber, Modelling the micro-climate of packed cut flowers during pre-cooling, in: Proceedings of the Nineteenth International Congress of Refrigeration, the Hague, Netherlands, 1995, pp. 707–714.

[14] R. Benzi, S. Succi, M. Vergassola, The lattice Boltzmann equation: theory and applications, Phys. Rep. 222 (3) (1992) 145–197.

[15] P. Bhatnagar, E.P. Gross, M.K. Krook, Phys. Rev. 94 (1954) 511.

[16] S. Chapman, T.G. Cowling, The Mathematical Theory of Non-Uniform Gases, Cambridge University Press, Cambridge, 1939.

[17] Y.H. Qian, D. d'Humieres, P. Lallemand, Lattice BGK models for Navier–Stokes equation, Europhys. Lett. 17 (6) (1992) 479–484.

[18] FIDAP v7.0, Fluid Dynamics International, Evanston, IL, USA, 1993.

[19] J.A. Somers, P.C. Rem, Flow computation with lattice gasses, Appl. Sci. Research 48 (34) (1991) 391–436.

[20] C. Kittel, Introduction to Solid State Physics, Wiley, New York, 1953.

[21] S.V. Patankar, Numerical Heat Transfer and Fluid Flow, Hemisphere, New York, 1980.

[22] M.R. Swift, E. Orlandini, W.R. Osborn, J.M. Yeomans, Lattice Boltzmann simulations of liquid gas and binary fluid systems, Phys. Rev. E 54 (5) (1996) 5041–5052.